British Columbia Geological Survey
Geological Fieldwork 1985

MINERALOGY AND METAL DISTRIBUTION HALLMAC MINE SANDON (82F/14, 82K/3)

By J. M. Logan
Department of Geological Sciences
The University of British Columbia

INTRODUCTION

Silver-lead-zinc ores have been produced from about 140 vein deposits in the Slocan mining camp since the 1890's. Discovery of the Hallmac deposit in August of 1980 marked the first significant discovery in the camp during recent years. The Hallmac mine is 1.7 kilometres north of Sandon in the centre of the camp (82F/14, 82K/3) (Fig. 45-1).

Supergene material accessible from surface pits accounted for early production of high-grade Hallmac ore. Bulk assays reported 127 ounces silver per ton, 72 per cent lead, 1.0 per cent zinc, and 0.02 ounce gold per ton for the initial 45-ton shipment (Goldsmith, 1981). Development continued sporadically for the next three years. The mine is closed at present.

This study was undertaken to examine metal and mineral distribution patterns within that part of the 'lode system' available for study. In addition, a comparative study was made of two spatially distinct mineralized veins, one along the footwall of the lode and the other along the hangingwall.

GENERAL GEOLOGY

The Late Triassic (Orchard, 1985) Slocan Group underlies the Sandon area in a structurally complex belt of typically argillaceous rocks with subordinate quartzite, limestone, and volcanic (tuffaceous) units. The principal structure within the camp is a regional recumbent fold concave to the southwest, referred to as the 'Slocan Syncline' (Hedley, 1952). Intruding the Slocan sediments, generally concordant with the strike of bedding, are dykes and sills related by Cairnes (1934) and Hedley (1952) to the Upper Jurassic Nelson batholith (Nguyen, *et al.*, 1968; Archibald, *et al.*, 1983). Emplacement of this composite, post-tectonic batholith (Duncan, *et al.*, 1979) has been related spatially and temporally by many (Cairnes, 1934; Reynolds and Sinclair, 1971; Cox, 1979; and Andrew, *et al.*, 1984) to the mineralizing event.

Slocan silver-lead-zinc-gold veins are mineralized parts of a system of interconnected and in many cases multistranded breaks or lodes (Robinson, 1950) which trend easterly to northeasterly across the regional fold structure of the enclosing strata. Veins occur along these lodes where dilation coincided in time with the mineralizing event(s).

MINE GEOLOGY

At the time of sampling the Hallmac lode had been developed over a horizontal length of 75 metres and vertical distance of 50 metres. Workings comprised two adit levels with the lode being explored by four subdrifts totalling nearly 250 metres in length (Fig. 45-2).

The predominant lithology encountered underground is massive argillite, in part shaly and thin bedded. Porphyritic dacite has intruded the sedimentary sequence concordant to bedding; dacite also locally occupies the lode structure, where it crosscuts bedding. Within the lode the dacite is typically pyritic; it is locally sheared and altered. Mineralization consists of massive pods and lenses of coarse-grained and local steel galena enclosed in a country rock of limonite-stained clay gouge. Trace amounts of sphalerite are also visible.

Following Cairnes' (1934) definition and classification scheme for mineralized structures in the Slocan camp, Hallmac is a 'shear-vein lode deposit' containing 'wet' ore. It comprises a roughly 10-metre-wide "lode" structure that strikes 075 degrees and is intermittently mineralized with lead, zinc, and silver sulphides. The geometry of the lode system is evident in vertical section A — A' (Fig. 45-3). Below 1735 level mineralization is confined to the walls of the shear zone, so separate hangingwall and footwall veins occur. Between these veins the lode is rarely mineralized and consists of variably sheared country rock. Above 1735 level the footwall is not well defined and the 'veins' appear to merge. Here the entire width of the lode consists of thoroughly sheared, altered country rock that contains relict stringers and pods of galena.

PETROLOGICAL SAMPLING PROCEDURES

Aggregate chip sampling of the mine was carried out during the summer of 1983. Later that same year additional sample rejects were supplied by the operators. Obviously, aggregate chip samples of this nature pose limits on textural and paragenetic studies, though at the outset of the study only a correlation between mineralogy and assay data was sought. In all, a total of 34 polished sections were prepared, 18 samples from the hangingwall vein and 16 from the footwall vein (Fig. 45-4).

A subset of five samples was selected to determine if redistribution of ore minerals during deformation could be related to microstructures. These samples were etched using either Brebrick and Scanlon (1957) etchant (following the technique of McClay, 1977) or a solution of $KMnO_4$ + H_2SO_4 (as outlined in Ramdohr, 1969) for galena and sphalerite respectively.

Mineralogy and paragenesis were established using a reflecting microscope and scanning electron microscope-energy dispersive X-ray emission spectrometer unit. Only a synopsis of the study results is presented here.

VEIN MINERALOGY

In the Hallmac deposit only galena with trace amounts of sphalerite and pyrite are visible mesoscopically. The gangue consists of crushed country rock, quartz, calcite, and siderite, all of which are thoroughly altered by supergene processes. No decrease in the amount of oxidation is evident with depth. Common vein mineralogy is galena, sphalerite, pyrite, freibergite, acanthite, pyrargyrite, chalcopyrite, and freieslebenite.

British Columbia Ministry of Energy, Mines and Petroleum Resources, Geological Fieldwork, 1985, Paper 1986-1.

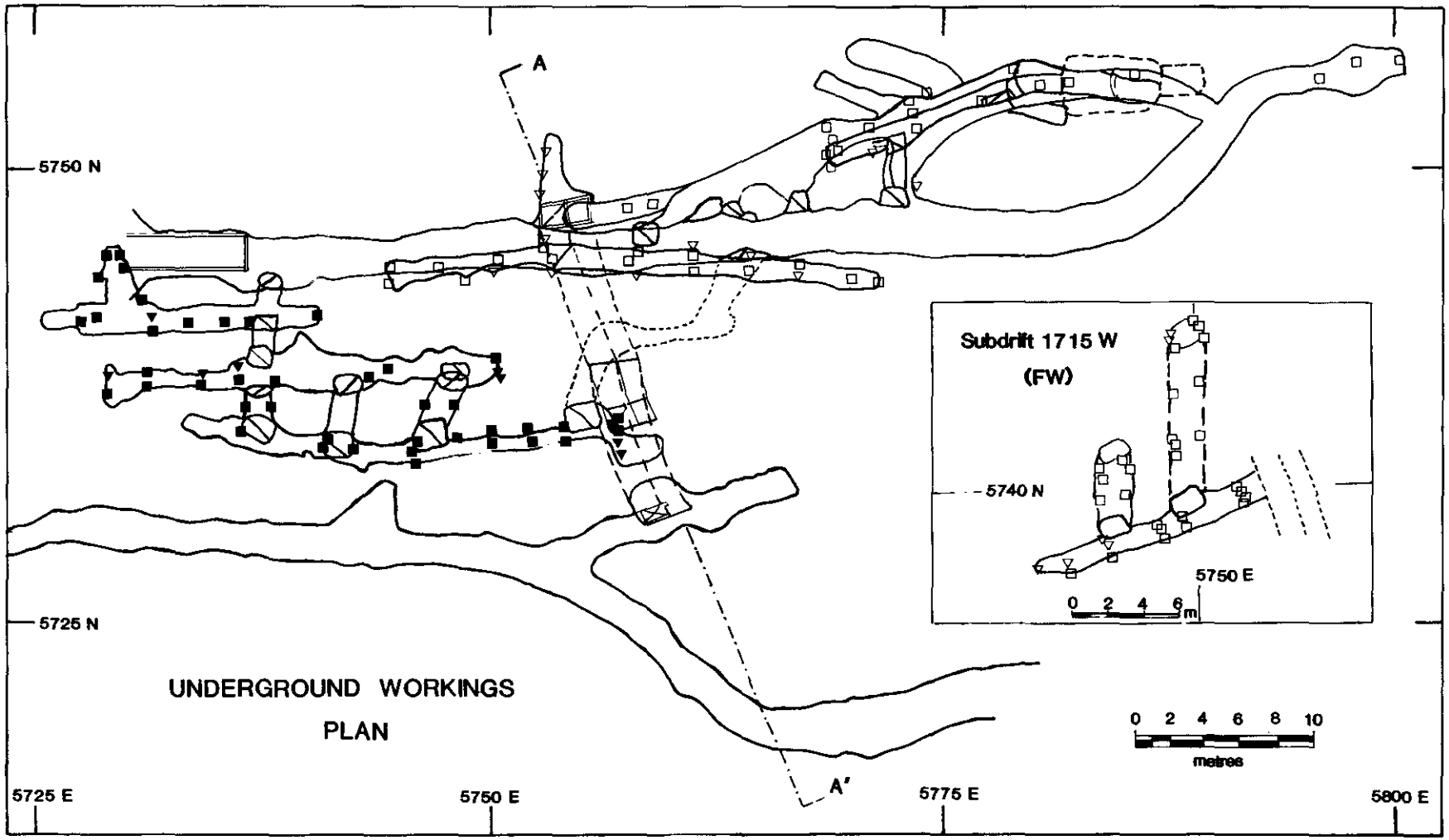

Figure 45-2. Plan view of underground workings, Hallmac mine, Sandon, showing location of single and composite samples. Symbols distinguish hangingwall vein (■) and wallrock (▼) from footwall vein (□) and wallrock (▼) samples.

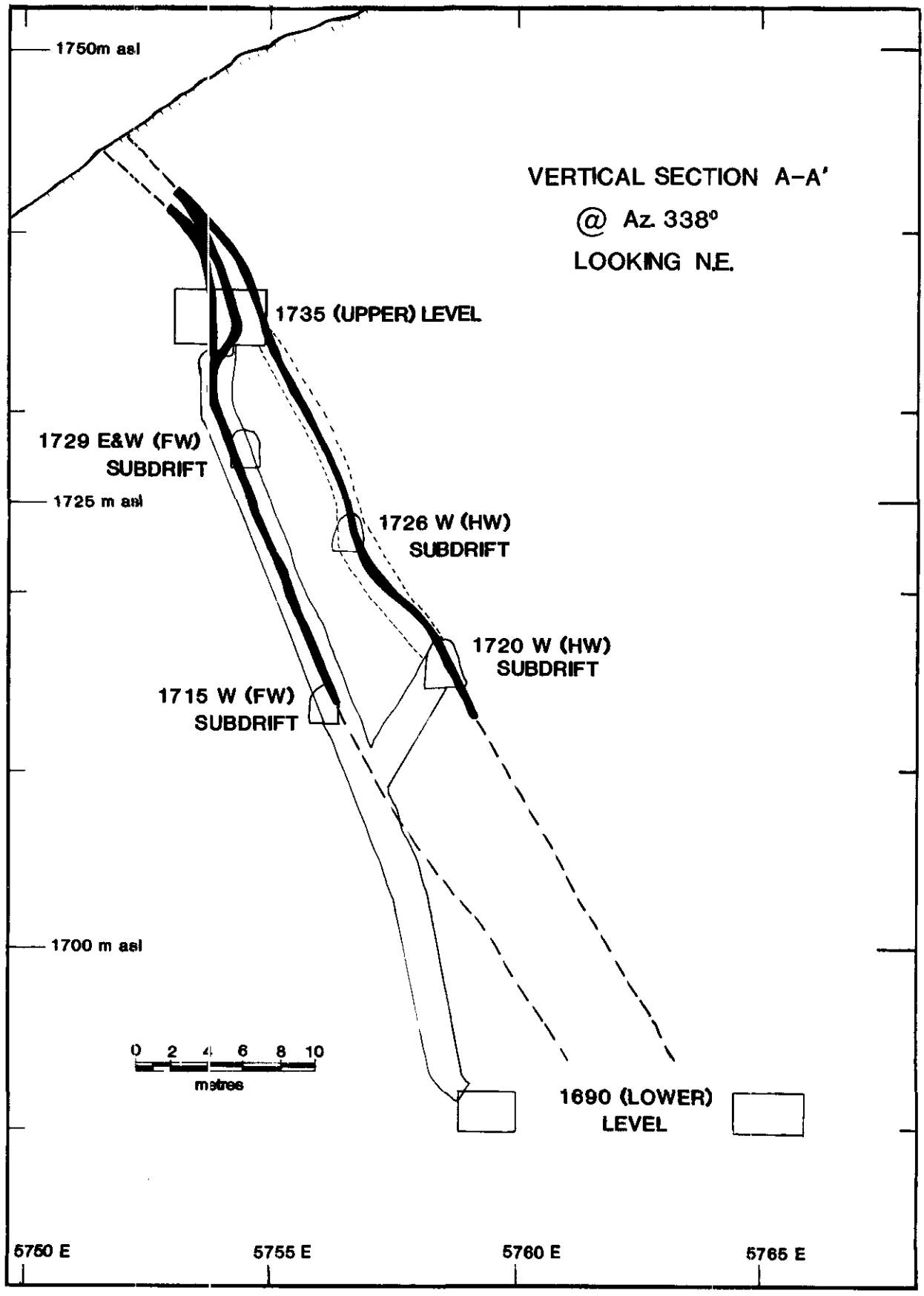

Figure 45-3. Vertical section A-A', Hallmac mine, Sandon, showing structure of lode system. Below the Upper level (1 735 metres above sea level) the structure branches into hangingwall and footwall veins.

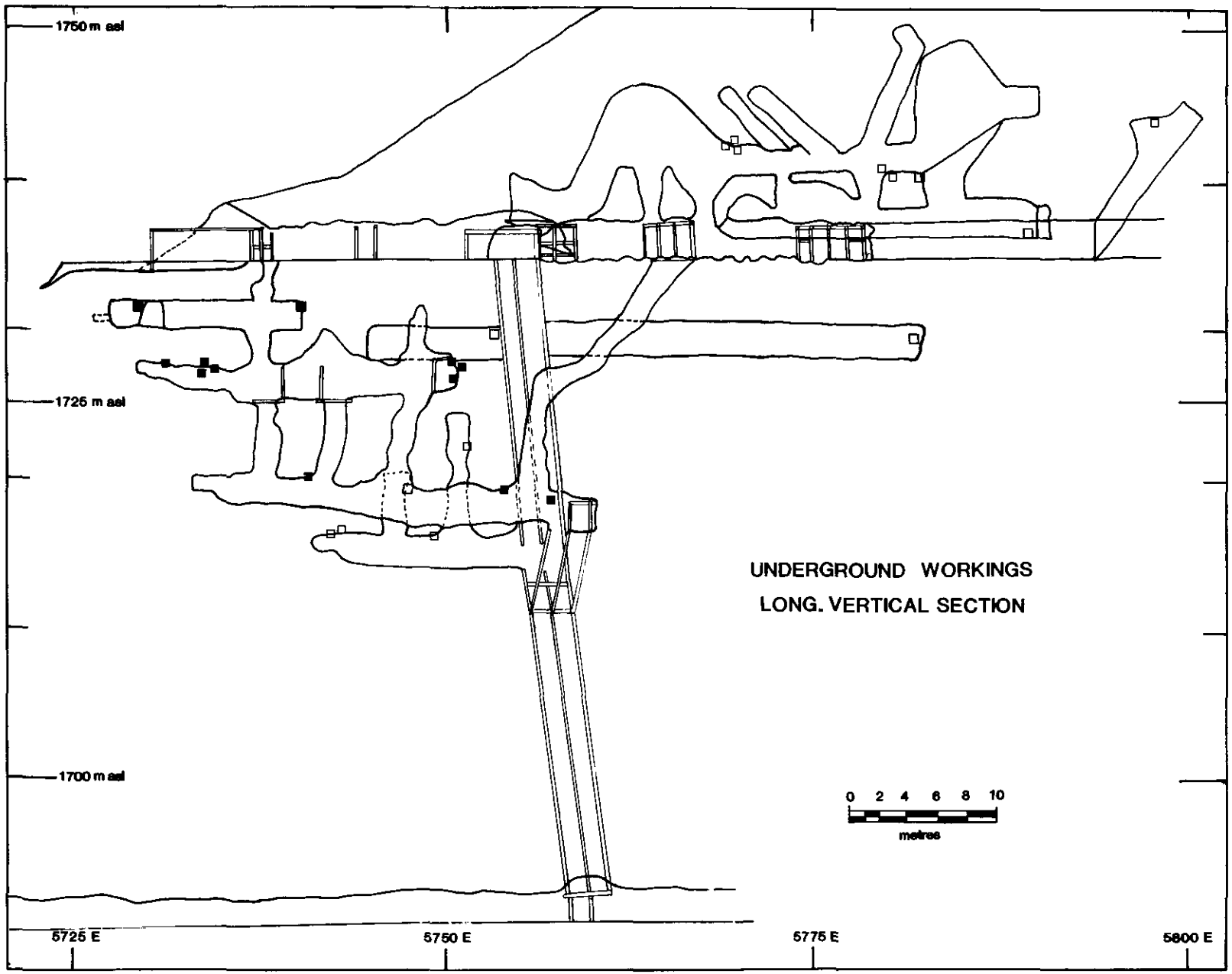

Figure 45-4. Longitudinal vertical section, Hallmac mine, Sandon, showing vertical and horizontal distribution of petrographic samples; hangingwall (■) and footwall (□).

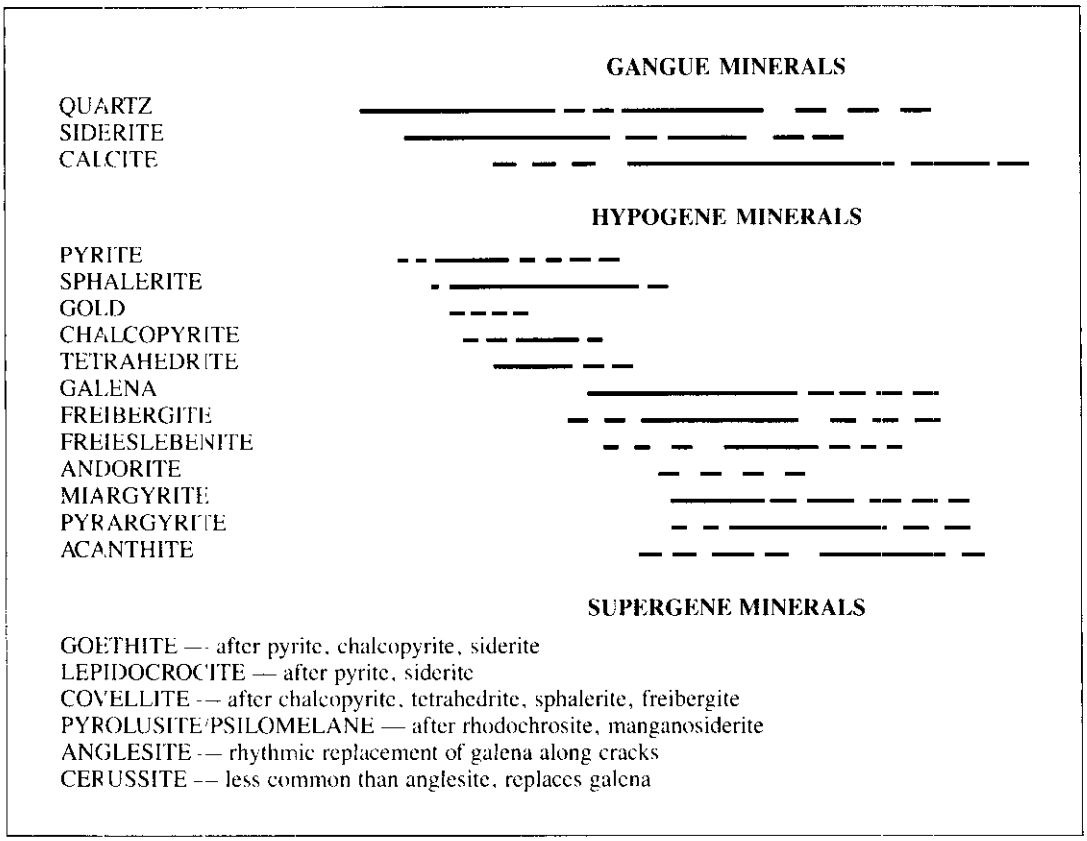

Figure 45-5. Paragenesis Hallmac mine line diagram.

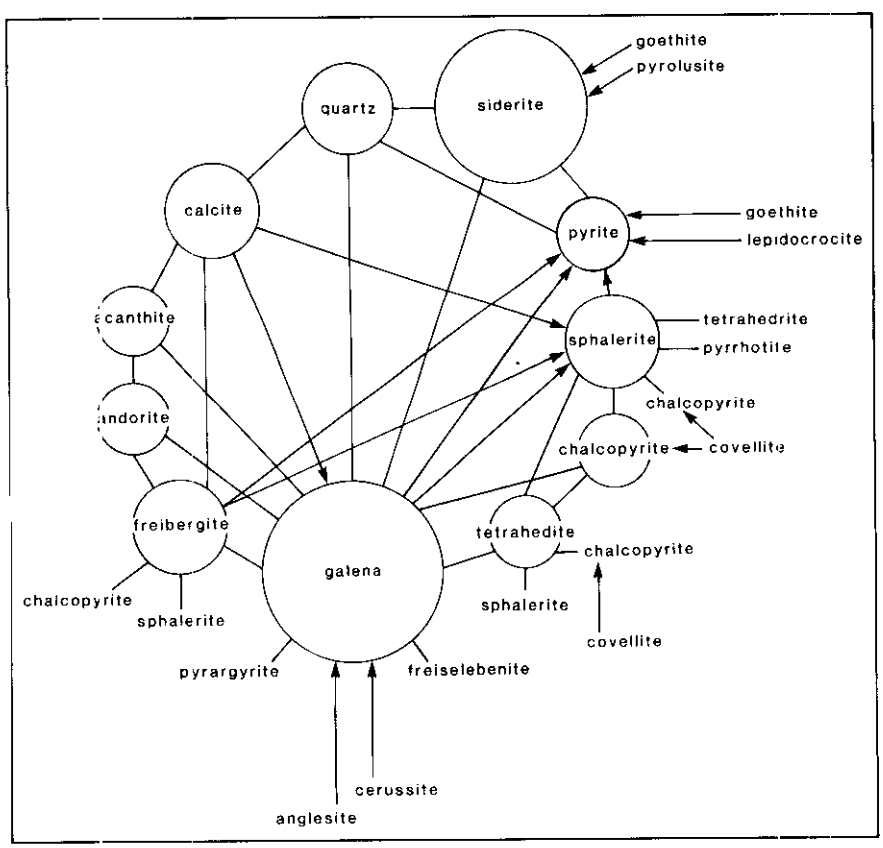

Figure 45-6. Van de Veer paragenetic diagram, Hallmac deposit.

MICROSTRUCTURES

Post-depositional shearing has affected the ore minerals variably, depending upon their respective rheologies and locations within the stress field. Pyrite has deformed by brittle fracture, and granulation has produced porphyroclasts of sphalerite. Where shearing has been operative both minerals are drawn out into parallel strings of granules within a matrix of galena (Plate 45-1).

Shearing has affected galena more noticeably than any of the other ore minerals. Grain size varies from coarsely crystalline (4 by 4-centimetre cubes) in zones isolated from shearing, to foliated steel galena where deformation has produced a variety of superimposed microstructures and textures in addition to grain size reduction. These textures include kink banding, polygonization, dynamic recrystallization and curved {001}cleavages. Kink band boundaries in galena are outlined by a high density of etch pits (= crystal dislocations) localized along slip planes (Plate 45-2b). Where polygonization developed adjacent to pyrite or sphalerite grains, small relict subgrains (Plate 45-2d) are preserved. Greater than 1 millimetre away from these areas of relatively high strain, subgrain size is markedly larger.

Freibergite and silver sulphosalts display different textures and residence following deformation. In samples which have undergone deformation these silver-bearing minerals occur in parallel layers intergrown with sphalerite, interstitial to polygonized galena, and localized along slip planes. In the undeformed samples, exsolution bodies of these minerals are aligned parallel to {100} planes in galena.

An increase in the grain size and relative abundance of freibergite and freieslebenite occur within deformed samples at the expense of oriented exsolution minerals. These 'second phase' inclusions are localized at triple junctions and along elongate grain boundaries coincident with partially annealed kink band boundaries.

PARAGENESIS

Relict depositional relations preserved in sheared samples and primary textures in unsheared samples permit a paragenesis to be determined with confidence, in contrast to the concerns of both Uglow (1917) and Bateman (1925). The paragenetic sequence of ore deposition for Hallmac follows closely that established by Cairnes (1934) for the Slocan camp, 'commencing with the earliest mineral: quartz, pyrite, calcite, siderite, sphalerite, grey copper, galena and argentite, pyrargyrite, silver'. The textural and paragenetic relationships for ore and gangue minerals is summarized in a line diagram (Fig. 45-5) and a Van de Veer diagram (Fig. 45-6).

Shearing and fracturing in not less than two separate events, likely syn and post-ore deposition, have altered the earliest formed textural relations. Uglow (1917) recognized 'gneissic galena' from Slocan ores to be a shear-generated texture and suggested that the *en echelon* distribution of orebodies within a shear zone was related to shearing parallel to an early vein. Ore shoot distribution, geometry, and mineral microstructures suggest a shear fracture origin. More recent studies (Atkinson, 1976; Clark, *et al.*, 1977; McClay and Atkinson, 1977) of the deformation and annealing properties for single galena crystals and polycrystalline aggregates have led to the quantification of deformation mechanisms and recovery processes.

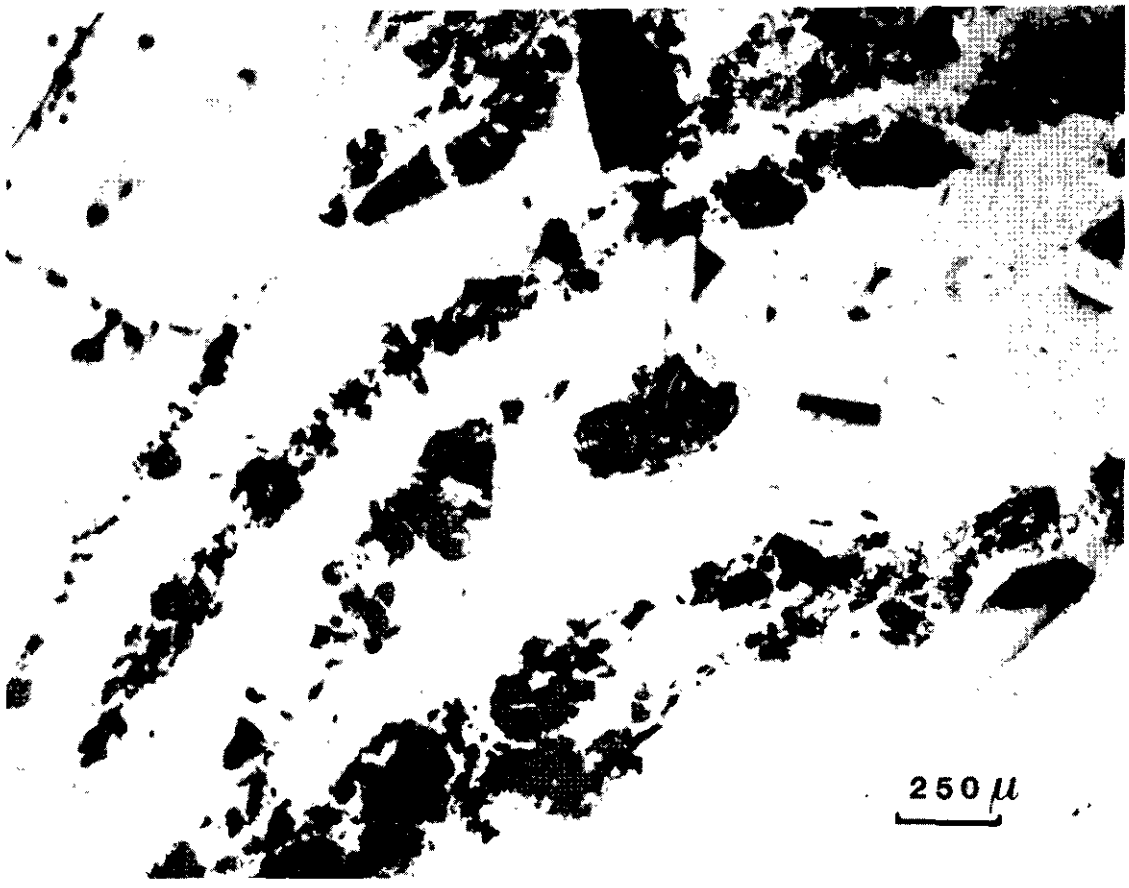

Plate 45-1. Parallel layers (dark) of sphalerite, freibergite, and pyrite granules defining mineral lineation in matrix of recrystallized galena (pale). Reflected plane polarized light.

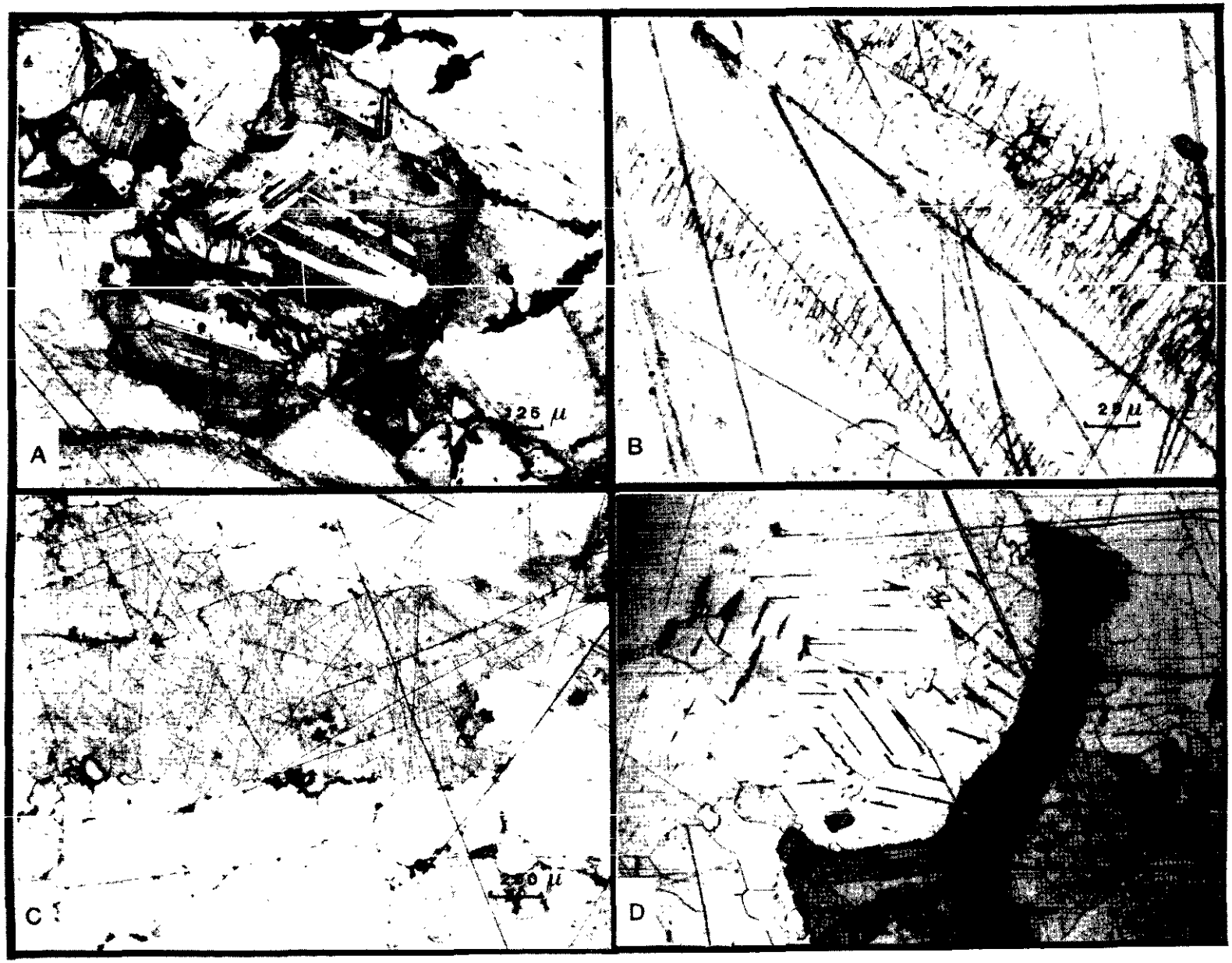

Plate 45-2. Reflected plane polarized light photomicrographs of polished and etched samples. A: Growth-annealing twins in sphalerite porphyroclasts (etched by $KMnO_4$ + H_2SO_4); B: Kink bands defined by etch pits (Brebrick and Scanion etchant); C: Sutured boundaries between elongate galena grains (etchant as in B); D: Sphalerite (centre) in groundmass of annealed galena. Freieslebenite occupies interstitial positions for foam texture. Relict subgrain evident in upper left (both Brebrick and Scanion etchant and $KMnO_4$ + H_2SO_4).

Interpretation of microstructures in light of these experimental studies allows constraints to be placed on the timing and mechanism of the redistribution of ore minerals.

Dynamic recrystallization (sutured boundaries on elongate grains, Plate 45-2c) and polygonization (Plate 45-2d) are common throughout deformed samples. Both are generated by intracrystalline deformation, neither requires later annealing (McClay, 1984). An upper temperature limit of 300 degrees Celsius (dry experimental deformation) is invoked by Clark, *et al.* (1977), as characteristic of 'sutured' kink band boundaries. Much lower temperatures are inferred for a fluid-dominated system such as is envisioned during the vein deposition episode.

Growth-annealing twins in sphalerite, locally pinned grain boundaries (calcite), and foam texture (120 degree triple junctions) in the most sheared samples are all indications of annealing processes. No restriction or systematic distribution between annealing textures versus deformation textures is obvious. Formation of annealed textures coincided with a period of high ambient temperature either metamorphic, hydrothermal, or shearing generated.

Recrystallization and microscopic redistribution of ore minerals occurred within the lode in response to tectonism. A simplistic approach to understanding the distribution of silver-bearing exsolution bodies in deformed samples was achieved by analysing small areas of the sample in terms of single crystal deformation mechanisms. Where the polycrystalline/polymineralic nature of the ore results in substantially more complex behaviour during deformation, this provides a working model for intragrain changes during deformation.

Nucleation sites of exsolution phases are localized at imperfections such as dislocations, twin lamellae, slip planes, and grain boundaries. Galena has two principal slip systems {100} <011> and {110} <110>; the former is operative below 300 degrees Celsius, and dislocation creep and glide are the deformation mechanisms (McClay, 1980). During low temperature deformation therefore, the slip and exsolution planes are coincident for galena. A dislocation climb-type mechanism is envisioned to facilitate migration from this plane of high stress to subgrain boundary locations. These inclusions alternatively may represent primary exsolutions involving no additional deposition.

Secondary or 'deformation induced' exsolution initiated by shear stress likely occurred during dynamic recrystallization and polygonization. This resulted in grain boundary migration and crystalliation of freieslebenite interstitial to galena subgrains. Exsolution minerals are impurities and as such cause deformation to take place at lower temperatures and/or lower stress. Hall and Czamanske (1975) reported similar mobilization and recrystallization of inclusions following gliding and resultant annealing in lead-silver ores from Idaho.

Late groundwater circulation along the lode structures has oxidized, leached, and further obliterated primary structures and produced supergene overprinting.

METAL DISTRIBUTION

ASSAY DATA

Data used to examine metal distribution patterns were collected and supplied to the writer by G. Salzar. The data comprises 150 chip samples distributed roughly equally between footwall and hangingwall veins. Samples were analysed by atomic absorption spectrophotometry at Loring Laboratories Ltd., Calgary, Alberta. The assay data include silver, lead, zinc, copper, and gold values and corresponding width measurements. Initial data were subdivided into hangingwall vein (n = 61), footwall vein (n = 73), and wallrock of both vein structures (n = 26). Assay results are not complete for either gold or copper. Sample coordinates were measured for each sample to permit machine contouring in plan and vertical section. Where more than one sample constitutes the width of the vein (at a single location) the disparity between samples is large in some cases. To facilitate contouring, such data were averaged and the mean replotted. This reduced the data set to n = 43 and n = 30 for footwall and hangingwalll samples respectively.

STATISTICAL ANALYSIS

Histograms and probability plots of both arithmetic and log values for all variables were computer generated. Silver, lead, and gold consist of mixtures of 3, 2, and 1 log-normal distributions respectively; zinc and copper consist of mixtures of 3 and 1 normal distributions respectively. Width was considered too subjective, considering the nature of these veins, and was not considered further.

Partitioning the data into the subpopulations described earlier was achieved graphically, following the procedure outlined by Sinclair (1976). Figure 45-7 illustrates the probability plot for silver from the hangingwall. Three populations are evident. The upper two with threshold values of 6 and 46 ounces silver per ton, correspond to 'mill-grade' and 'high-grade' ore respectively. The means, standard deviations, and threshold values for partitioned populations of silver, lead, zinc, copper, and gold are presented in Table 45-1. The threshold values provide the contour values which separate and define high-grade ore shoots (population A) and separate mineral zoning patterns.

TRIANGULAR PLOTS

Goldsmith (1984) has shown the usefulness of triangular plots in characterizing metal ratios of deposits in individual mining camps. Here plotting assay data on triangular plots permits recognition of separate data clusters within a single deposit. The most useful triangular plots for examining fundamental differences in metal

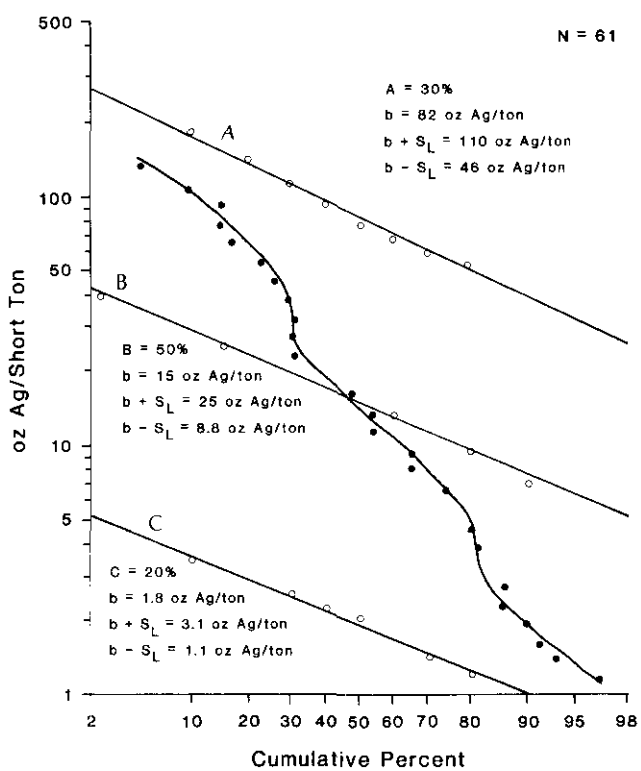

Figure 45-7. Probability graph for 61 silver values from hangingwall vein. Black dots are original data, open circles are estimated partitioning points. Three populations are evident from lognormal distribution of silver values.

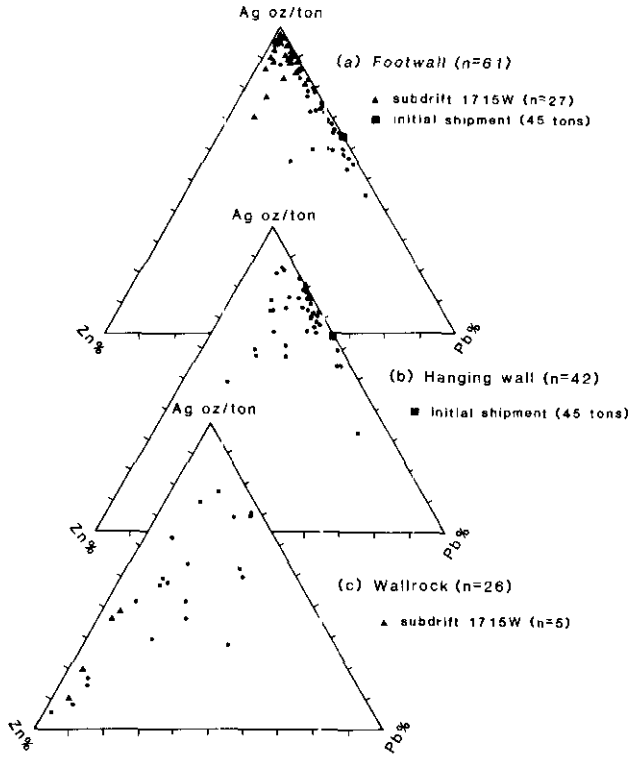

Figure 45-8. Silver-zinc-lead triangular plots of footwall, hangingwall, and wallrock, Hallmac mine.

ratios in Hallmac assay data are silver-zinc-lead and copper-silver-lead. To produce more easily interpreted patterns, copper and gold data were converted to ppm/100. Silver is plotted as ounces per ton and lead and zinc as per cent.

Silver (ounces)-zinc (per cent)-lead (per cent) plots for footwall and hangingwall data sets (Fig. 45-8) indicate that: silver-lead ratios for veins (and wallrock) generally exceed 1 ounce/per cent; zinc is subordinate to lead, as for Trout Lake camp (Goldsmith, 1984); and a subset of the footwall data contains high silver to lead ratios. Comparison of Figure 45-8a with Figure 45-9b indicates a subgroup of 27 samples with silver-lead ratios exceeding 4 ounces silver/1 per cent lead. Examination of samples from subdrift 1715 W shows that 25 of the 29 were collected from this one small area. Once subdrift 1715 W is isolated, distinctions between hangingwall and footwall become less evident. Figure 45-8 indicates slightly higher relative silver and zinc in the hangingwal samples compared with those for the footwall.

Figure 45-8c shows that plots of metal ratios in wallrocks exhibit considerable scatter; a continuous variation in proportions extends from the mineralized vein field to the zinc vertex; and lead is generally subordinate to zinc. A small group of five samples contains similar proportions but lower absolute amounts of silver-zinc-lead than average vein samples. This apparent overlap emphasizes the difficulty in separating vein from wallrock, particularly where post-ore deformation has obscured the contacts. No apparent supergene enrichment of silver values is evident for wallrock from subdrift 1715 W.

The zinc-copper-lead plot (Fig 45-9a) shows two clusters of data where lead values are subordinate to zinc (a characteristic typical of wallrocks). The cluster near the copper vertex corresponds to a footwall subset representing subdrift 1715 W. A hangingwall copper-zinc-lead plot shows a similar cluster of data, which corresponds to sample sites located in the lowest portions of the hangingwall workings. This area coincides roughly in elevation with subdrift 1715 W.

A silver-copper-lead plot does not produce a clearly defined footwall subset, instead the data tend to spread out close to the silver-copper line in response to the low relative lead abundance of the data (Fig. 45-9b).

PLAN AND VERTICAL CONTOURING

Composite plans, rather than individual level plans, have been constructed for silver, lead, zinc, copper, and gold utilizing the entire assay database. For this, data from all levels including hangingwall, footwall, and wallrock samples (n = 150) were projected to one plane and contoured. Threshold values defined in Table 45-1 were used as the initial contour values. The more common practice of compiling level plans proved unsatisfactory because of small data sets reflecting the limited size of the workings. These plots (not reproduced here) illustrate the general east-west strike of the fissure and the gross geometry of assay-defined ore shoots, the southwesterly rake of which is the most apparent feature.

Simple correlation between elements and zonation patterns are best illustrated on vertical sections. Using respective assay data from either footwall or hangingwall structures, east-west vertical sections for both were constructed. The variables included the same five metals listed previously and, in addition, various metal ratios. Figure 45-10 shows contoured log silver values for the hangingwal workings. Overlaying log 10 × lead (population A) and log 100 × zinc (populations A and B) contours, it is evident that silver and lead are positively correlated. Zinc is peripheral to both silver and lead

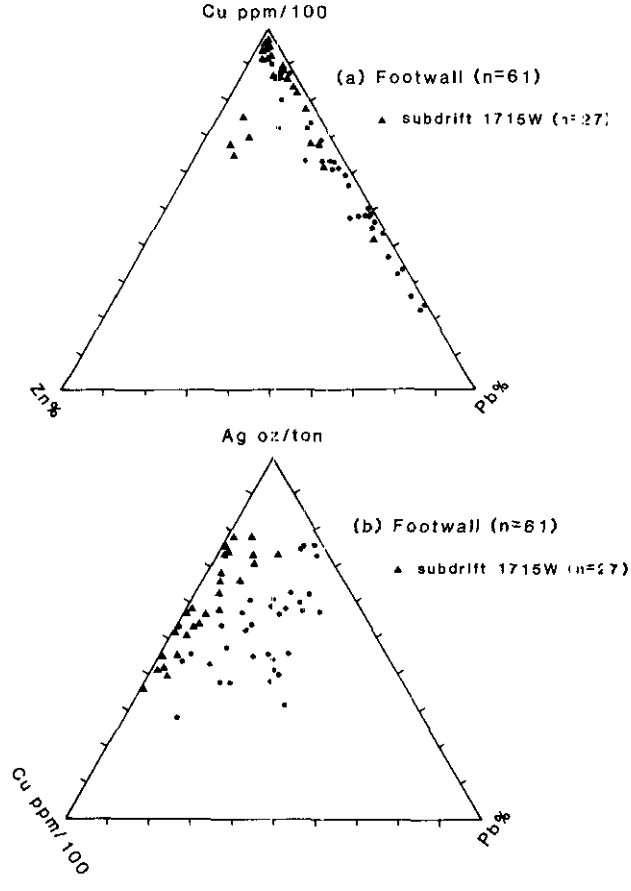

Figure 45-9. Zinc-copper-lead and silver-copper-lead triangular plots of footwall, Hallmac mine.

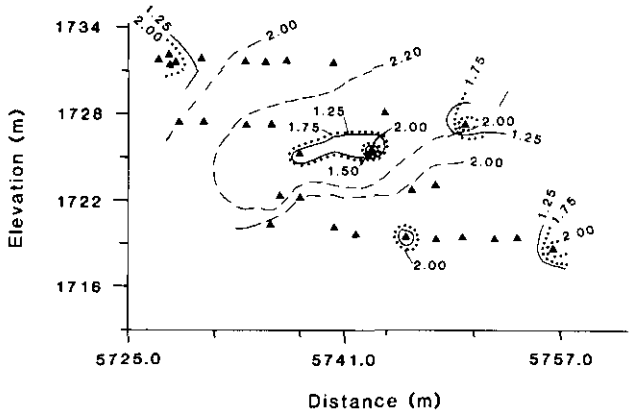

Figure 45-10. Hangingwall vertical section. Dashed contour lines are log (100 × Zn per cent); dotted lines log Ag (ounces per ton); and solid lines log (10 × Pb per cent). Zinc outlines a concentric central zone cored by high-grade silver and lead. Silver and lead show coincident distribution and define ore shoot locations throughout the workings.

and outlines a concentric zone of high values centred on the hangingwall workings. The same pattern for silver and lead is found in the footwall vertical section, though that for zinc is less apparent.

Subdrift 1715 W data, which forms a separable cluster on triangular plots, was isolated from the footwall and contoured separately (Fig. 45-11). Plotting single metals shows that highest silver and lead values coincide with the uppermost sections of both raises and the west end of the subdrift. Contouring silver suggests two >50-ounce-per-ton silver zones raking 30 degrees southeast. Lead values decrease down rake away from the 'silver-defined' shoots. Contour patterns for both zinc and copper are less consistent, showing no systematic distribution. Higher values for both metals coincide in part with the ore shoots, but just as commonly do not.

Contour plots of logged lead to zinc ratios show that values decrease down rake, away from the ore shoots. The reverse is true for logged silver to lead ratios: these values increase by an order of magnitude proceeding from the upper to lower portions of the workings (Fig. 45-11c). Logged silver to zinc ratios (Fig. 45-11d) define a central, westerly raking low perpendicular to the rake of the ore shoots, thus defining limits to the down rake extension of the >50-ounce-per-ton silver ore shoots.

DISCUSSION

Metal zoning patterns in individual ore shoots, noted first by Cairnes (1934), have been the focus of re-interpretation by numerous later studies (Robinson, 1948; Hedley, 1952; Orr, 1971). The pattern is described as a vertical phenomenon characterized by galena and silver minerals in the uppermost sections, surrounded by a sphalerite-rich zone, which gives way successively downward to pyritic and silicic zones. Cairnes (1934) attributed this pattern to a steep geothermal gradient coincident with the present topography. Hedley (1952) and Robinson (1948) suggested mineral precipitation to be a pressure-related phenomena, relating zonation to vein dilation which in turn was related to closeness to the surface. Orr (1971), using production data and elevation of Slocan City deposits to the south, could not identify vertical zoning within individual deposits, although he documented a district zonation for the Slocan City camp.

Traditionally this zoning pattern has been viewed as unidirectional and not concentric. From top to bottom the pattern is identical to the paragenetic sequence for the camp and early workers cited this to support a granitic source for the deposits. Hedley (1952)

TABLE 45-1
MEANS, STANDARD DEVIATIONS, AND THRESHOLDS DETERMINED GRAPHICALLY FOR PARTITIONED METAL VALUES

	FOOTWALL VEIN					HANGINGWALL VEIN				
Element Unit	Populations Per Cent	b[1]	b+s[2]	b−s[3]	Thresholds	Populations Per Cent	b[1]	b+s[2]	b−s[3]	Thresholds
Ag	A(0.59)	60	110	32	45	A(0.30)	82	110	46	46
Oz./ton					25					17
	B(0.33)	12	22	6.8	5.5	B(0.50)	15	25	8.8	6.0
	C(0.08)	3	4.1	2.1		C(0.20)	1.8	3.1	1.1	
Pb	A(0.80)	9.8	30	2.8	3.0	A(0.42)	21	36	12	20
Per cent					0.8					7.0
	B(0.20)	0.62	1.3	0.3		B(0.58)	1.8	5.8	0.54	
Zn[4]	A(0.03)	2.37	2.42	2.32	2.2	A(0.05)	2.6	2.7	2.5	2.37
Per cent	B(0.15)	1.72	1.95	1.47	1.7	B(0.57)	1.4	1.8	0.97	1.05
					1.25					0.5
	C(0.82)	0.92	1.3	0.52		C(0.38)	0.55	0.78	0.30	
Cu[4]	A(1.0)	0.175	0.33	0.04	0.45	A(0.08)	0.35	0.39	0.31	0.28
Per cent						B(0.52)	0.15	0.21	0.09	0.10
										0.03
						C(0.40)	0.08	0.07	0.02	
Au Oz./ton	A(1.0)	0.0057	0.022	0.0014	0.08	A(1.0)	0.0076	0.026	0.0023	0.08

Per cent of data in population.
[1]Antilog of mean of log-normal population.
[2]Antilog of mean plus one standard deviation of log-normal population.
[3]Antilog of mean minus one standard deviation of log-normal population.
[4]Normal distribution.

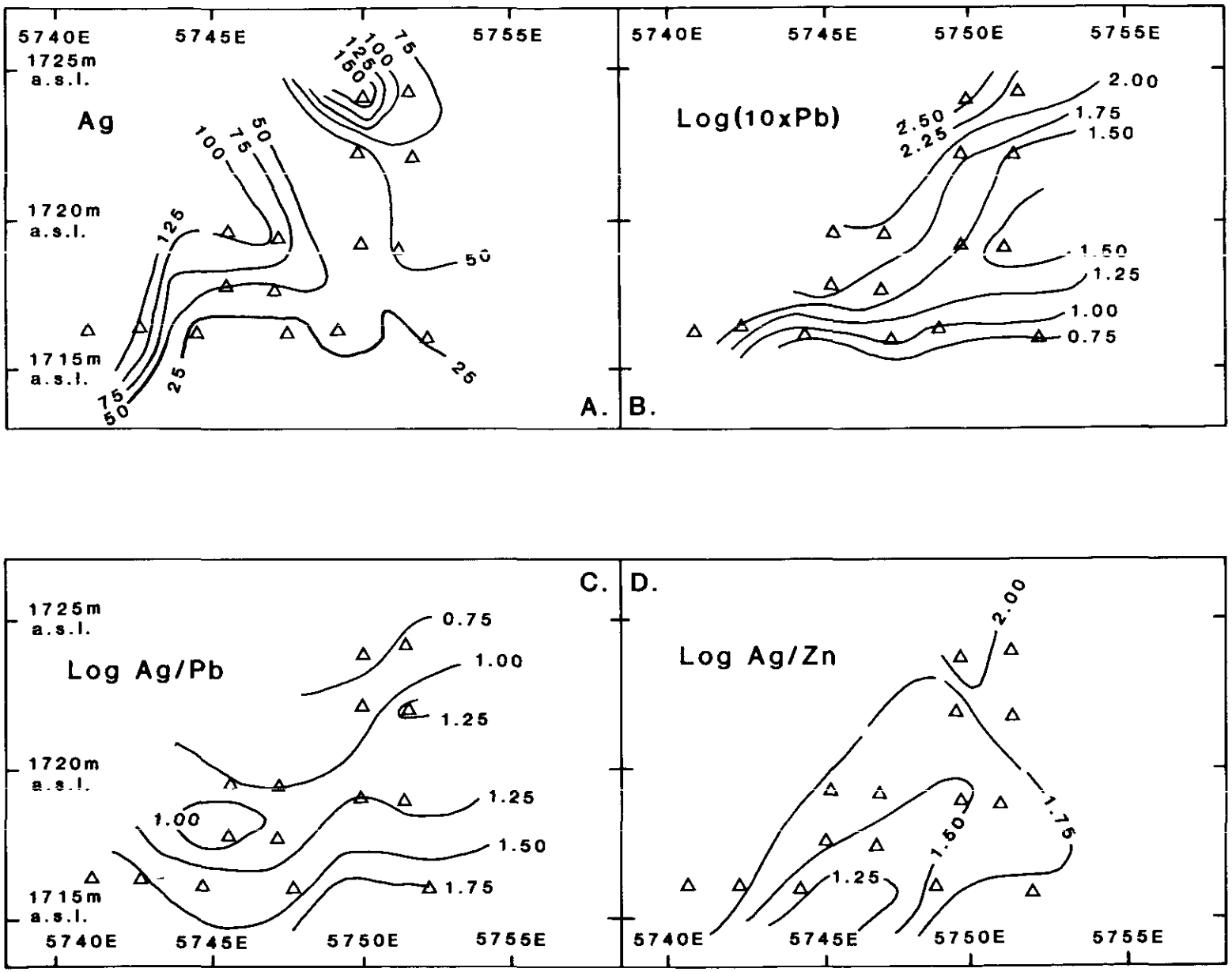

Figure 45-11. Contoured assay values for subdrift 1715 W. Triangles give data points. A: silver in ounces per ton; B: log (10 x Pb) in per cent; C: log Ag/Pb ratios, silver in ounces per ton and lead in per cent, D. log Ag/Zn ratio with silver in ounces per ton and zinc in per cent.

discussed lateral continuity within lode structures and suggested a concentric zoning pattern. Ideally, mineral deposition in a dilation structure should produce a concentric zoning pattern which reflects the paragenesis. The earliest minerals adjacent to vein walls and the latest in the centre or core. Missing zones would reflect intermittent closures of the structure that restricted fluid flow.

Triangular plots have been shown effective on a single deposit scale in defining separate groups of data. Such plots utilize proportions rather than absolute amounts of three elements. Thus, where strong correlation exists between the elements, little or no distinction is made between high-grade or low-grade samples. Discrimination between slightly mineralized wallrock and low-grade vein material or waste is possible on the basis of relative proportions, particularly silver, lead, and zinc. Using either relative proportions or selective metal ratios, 'discriminant areas' could be defined for triangular plots. These areas would correspond to specific zones within the ideal zonation pattern for Slocan ore shoots and provide a more predictive alternative for locating ore shoots. Historically silver values alone have directed underground exploration.

Contouring assay data allows recognition of generalized metal associations and spatial distributions within the Hallmac deposit. Analysis of Hallmac metal distribution patterns, following Sinclair and Tessari's method (1980), indicates a generalized zonation pattern compatible with the established paragenesis. The method involves arranging samples in order of decreasing values of a key metal; in this study both silver and zinc were tested. Other element distributions are examined relative to this idealized ordering of one element. Upper population (A) values correspnding to high-grade ore shoots reflect a simple zonation model of high zinc values peripheral to or enveloping a high silver and lead core. This zonal pattern does not extend beyond the scale of ore shoots for either footwall or hangingwall data.

Contoured ratios of metal pairs for both hangingwall and footwall structures show a distinctive zonation pattern for subdrift 1715 W. This departure from the generalized 'wet-ore' zonation pattern suggests either a separate silver mineralizing event of enrichment or nonsymmetric overlap of zonation patterns. Contouring the data indicates that high ratios in which log (silver/lead) exceeds 1 are localized at the fringes of ore shoots where average ratios are 1. Comparing absolute values of silver and lead indicates only lower average lead rather than higher silver for subdrift 1715 W. Silver values extend outward from this silver-lead core, likely in the form of late-stage silver-bearing minerals. The lower than average abundance of galena is evident in polished aggregate sections from 1715 W subdrift, where half of the samples contained few visible sulphides of any type. Pyrargyrite and acanthite have replaced both galena and locally calcite, suggesting a late stage of predominantly silver mineralization. An equally plausible explanation for apparent enrichment of silver and copper with respect to lead is supergene enrichment.

CONCLUSIONS

Hallmac deposit contains the mineralogy typical of Cairnes' 'wet-ore' classification. Mineralogical and paragenetic studies have established the presence of pyrite-sphalerite-galena and a complex assemblage of silver minerals. Early and late stages of silver mineralization are characterized by distinctive mineralogies and are separable by their respective metal zoning patterns. Observed textures and distribution patterns of early freibergite and silver sulphosalts indicate an exsolution origin in galena. Late-stage silver minerals, pyrargyrite, andorite, and acanthite, postdate the bulk of galena deposition; thus, replacement of galena and overprinting of earlier developed zoning patterns typify this younger stage of silver mineralization.

Early-stage silver-sulphosalt textures indicate exsolution following an initial precipitation as some PbS-Ag_2S-Sb_2S_3 solid solution. Exsolution laths of freieslebenite in galena suggest a temperature of deposition of about 350 degrees Celsius (Hoda, *et al.*, 1975).

Sulphide microstructures within the lode indicate redistribution of minerals on both a macro and microscopic scale related to ductile deformation and annealing processes. Exsolution minerals in galena are most affected.

Statistically defined contour values (thresholds) clearly identify a zonal distribution of sulphides in ore shoots. These patterns illustrate the 'classic' camp zoning pattern, developed for single ore shoots. Ratios of metal pairs isolate subdrift 1715 W as different from the generalized zonal pattern.

Triangular plots of metal abundances are also effective in distinguishing vein material in subdrift 1715 W from the rest of Hallmac deposit. The 1715 W data cluster close to the silver vertex on the silver-zinc-lead plot indicating relatively higher silver and lower lead than the remainder of the data. With the exception of lead, absolute metal values for subdrift 1715 W are comparable in range and proportion (A:B:C populations) with the rest of the footwall data. Lead values are an order of magnitude lower, but do not account solely for the relative increase in silver. Polished sections indicate less galena and related sulphosalts and a greater proportion of pyrargyrite and argentite. This suggests that late-stage silver mineralization took place in the 1715 W drift area of the mine.

ACKNOWLEDGMENTS

This study has been supported by research funds from Arctex Engineering Ltd. and the Natural Science and Engineering Research Council of Canada to A. J. Sinclair. The cooperation of Hallmac Mines Ltd. and their consultant, Guy Salazar, is appreciated.

REFERENCES

Andrew, A., Godwin, C. I., and Sinclair, A. J. (1984): Mixing Line Isochrons: A New Interpretation of Galena Lead Isotope Data from Southeastern British Columbia, *Econ. Geol.*, Vol. 79, pp. 919-932.

Archibald, D. A., Glover, J. K., Price, R. A., Farrar, E., and Carmichael, D. M. (1983): Geochronology and Tectonic Implications of Magmatism and Metamorphism, Southern Kootenay Arc and Neighbouring Regions, Southern British Columbia, Pt. I, Jurassic to mid-Cretaceous, *Cdn. Jour. Earth Sci.*, Vol. 20, pp. 1891-1913.

Atkinson, B. K. (1976): Deformation Mechanism Maps for Polycrystalline Galena, *Earth and Planet. Sci. Lett.*, Vol. 29, pp. 210-218.

Bateman, A. M. (1925): Notes on Silver-lead Deposits of Slocan District, British Columbia, Canada, *Econ. Geol.*, Vol. 20, pp. 554-572.

Brame, S. (1979): Mineralization near the Northern Margin of the Nelson Batholith, M.Sc. Thesis, *University of Alberta*, Edmonton, 146 pp.

Brebrick, R. F. and Scalon, W. W. (1957): Chemical Etches and Etch Pit Patterns on PbS Crystals, *Jour. Chem. Physics*, Vol. 27, pp. 607, 608.

Cairnes, C. E. (1934): Slocan Mining Camp, British Columbia, *Geol. Surv., Canada*, Mem. 173, 137 pp.

Clark, B. R., Price, F. R., and Kelly, W. C. (1977): Effects of Annealing on Deformation Textures in Galena, *Contributions to Mineralogy and Petrology*, Vol. 64, pp. 149-165.

Cox, J. (1979): The Geology of the Northwest Margin of the Nelson Batholith, British Columbia, M.Sc. Thesis, *University of Alberta*, Edmonton, 95 pp.

Duncan, I. J., Parrish, R. P., and Armstrong, R. L. (1979): Rb/Sr Geochronology of the Post-tectonic Intrusive Events in the Omineca Crystalline Belt, Southeastern British Columbia (abstract), Cordilleran Section, *Geol. Assoc. Canada*, Vancouver, *Program and Abstracts*, p. 15.

Goldsmith, L. B. (1984): A Quantitative Analysis of Some Vein-type Mineral Deposits in Southern British Columbia, M.Sc. Thesis, *University of B.C.*, Vancouver, 86 pp.

Goldsmith, L. B. (1981): High-grade Silver-lead Discovery, Summary of Exploration Activities, 1980 Hall Mineral Claim Group, Slocan Mining Division, Sandon, British Columbia, private rept. prepared for *Hallmac Mines Ltd.*, 30 pp.

Hall, W. E. and Czamanske, G. K. (1972): Mineralogy and Trace Element Content of the Wood River Lead-silver Deposits, Blaine County, Idaho, *Econ. Geol.*, Vol. 67, pp. 350-361.

Hedley, M. S. (1952): Geology and Ore Deposits of the Sandon Area, Slocan Mining Camp, British Columbia, *B.C. Ministry of Energy, Mines & Pet. Res* , Bull. 29, 130 pp.

Hoda, S. N. and Chang, L.L.Y. (1975): Phase Relations in the Systems PbS-Ag_2S-Sb_2S_3 and PbS-Ag_2S-Bi_2S_3, *Amer. Mineral.*, Vol. 60, pp. 621-623.

McClay, K. R. (1977): Dislocation Etch Pits in Galena, *Tectonophysics*, Vol. 40, T1-T8.

———— (1980): Sheared Galena; Textures and Microstructures, *Jour. Struct. Geol.*, Vol. 2, No. 1/2, pp. 227-234.

———— (1984): Structural Geology of Stratiform Lead-zinc Deposits: Case Histories, *Geol. Assoc. Canada*, Cordilleran Section, Short Course No. 2 (Pt. II), 150 pp.

McClay, K. R. and Atkinson, B. K. (1977): Experimentally Induced Kinking and Annealing of a Single Crystal of Galena, *Tectonophysics*, Vol. 39, pp. 175-189

Nguyen, K. K., Sinclair, A. J., and Libby, W. G. (1968): Age of the Northern Part of the Nelson Batholith, *Cdn. Jour. Earth Sci.*, Vol. 5, pp. 955-957.

Orchard, M. J. (1985): Carboniferous, Permian and Triassic Conodants from the Central Kootenay Arc: Constraints on the Age of the Milford, Kaslo and Slocan Groups, *in* Current Research, Pt. A, *Geol. Surv., Canada*, Paper 85-1A, pp. 287-300.

Orr, J.F.W. (1971): Mineralogy and Computer-oriented Study of Mineral Deposits in Slocan City Camp, Nelson Mining Division, British Columbia, M.Sc. Thesis, *University of B.C.*, Vancouver, 143 pp.

Ramdohr, P. (1969): The Ore Minerals and Their Intergrowths, *Pergamon Press*, New York, 1174 pp.

Reinsbakken, A. (1968): Fluid Inclusion Studies of Gangue Minerals from the Slocan Mining District, British Columbia, B.Sc. Thesis, *University of B.C.*, Vancouver, 73 pp.

Reynolds, P. H. and Sinclair, A. J. (1971): Rock and Ore-lead Isotopes from the Nelson Batholith and the Kootenay Arc, British Coumbia, Canada, *Econ. Geol.*, Vol. 66, pp. 259-266.

Robinson, M. C. (1948): An Analysis of the Depth Problem in the Slocan Mining Camp, British Columbia, B.Sc. Thesis, *University of B.C.*, Vancouver, 98 pp.

———— (ca. 1950): Geological Setting and Relationships of the Silver-lead-zinc Ore Deposits of the Silverton Area, Slocan Mining Camp, Unpub. Rept.

Sinclair, A. J. (1976): Application of Probability in Mineral Exploration, Sp. Vol. No. 4, *Assoc. Explor. Geochem.*, Richmond B.C., 95 pp.

Sinclair, A. J. and Tessari, O. J. (1980): Vein Geochemistry, an Exploration Tool in Keno Hill Camp, Yukon Territory, Canada, *Jour. Geochem. Explor.*, Vol. 14, pp. 1-24.

Uglow, W. L. (1917): Gneissic Galena Ore from the Slocan District, British Columbia, *Econ. Geol.*, Vol. 12, pp. 643-662.